

THE APPLICATION OF SIMULTANEOUS DTA AND TG TO SOME ASPECTS OF OIL SHALE MINERALOGY

S.ST.J. WARNE and D.H. FRENCH

Department of Geology, The University of Newcastle, N.S.W. 2308 (Australia)

(Received 6 December 1983)

ABSTRACT

The mineralogy of most Australian oil shales is relatively simple and belongs to the carbonate, clay, sulphide, sulphate, silica, phosphate, zeolite and evaporite/saline mineral groups.

Retorting involves heating during which virtually all oil shale minerals react. Such reactions, endothermic or exothermic may be characterised and measured by DTA, whilst associated weight variations may be continuously quantified by TG. These methods provide mineralogical identification and evaluation data, together with reaction type, magnitude and heat balance information, obtained under heating rate and gas atmosphere conditions preselectable to simulate various retorting conditions.

Endothermic and exothermic mineral reactions taking place within the retort may strongly influence the required retort heat balance regime. Detailed knowledge of the actual minerals present, their quantities, reaction temperatures and types, together with heat balance effects are of marked technological importance to the design and operation of oil shale retorts and the assessment of spent shale characteristics and potential utilisation.

INTRODUCTION

The group of solid hydrocarbon rich sediments of variable composition collectively classified as oil shales, constitute a major alternative source of hydrocarbons. These sediments, usually as mined, although beneficiation may be practical, are heated to drive off the recoverable liquid and gaseous hydrocarbon contents. This heating aspect immediately highlights the potential use of thermal analysis techniques for the thermal and utilisation characterisation of both the organic and inorganic mineral components of oil shale. It is noteworthy that the mineral constituents and their proportions are likely to vary most within a particular oil shale deposit. In addition to simple dilution such mineralogical variations may negatively influence the hydrocarbon yield due to adverse endothermic effects [1] or the presence of specific minerals [2].

The mineralogy of most Australian oil shale deposits, investigated to date, is relatively simple [3–5]. The constituent components belong to the carbonate, clay, sulphide, sulphate, silica, phosphate, zeolite and evaporite/saline mineral groups. Although too early yet to judge, the information available from elsewhere tends to indicate that mineralogically “typical” oil shales may be relatively simple in comparison to the Green River oil shales (U.S.A.), in which some 70 authigenic minerals occur. These range from common to rare, include several new minerals and a considerable number of different carbonates [6].

Virtually all these minerals react, in some way, on heating, e.g., by decomposition, intermineral or decomposition product reactions, oxidation, reduction, crystallographic changes or melting. All such reactions are either endothermic or exothermic (occasionally reversible) and may be detected and characterised by differential thermal analysis (DTA), while associated weight variations (gains or losses) may be continuously measured by thermogravimetry (TG). The resultant continuously recorded thermal analysis curves provide methods for mineral identification and evaluation together with the reaction type, magnitude and heat effects produced under preselected heating rate and gas atmosphere conditions, which may be varied to simulate various retorting conditions.

The specific atmosphere composition conditions, temperatures and temperature gradients needed during retorting for maximum hydrocarbon extraction are maintained at the expense of some of the yield gas which is fed back into the combustion zone and burnt. In this context the endothermic or exothermic oil shale mineral reactions taking place within the retort charge will clearly influence the required optimum heat regime, e.g., as oil shales contain considerable mineral matter contents (usually in excess of 50%), the effects under oxidising conditions of the decomposition of high contents of calcite (CaCO_3) or siderite (FeCO_3) would be strongly endothermic to moderately exothermic, respectively [7].

Thus, a detailed knowledge of the actual minerals present, their quantities, reaction temperatures and mechanisms, together with heat balance effects are therefore of technological importance in the design and operation of oil shale retorts.

Furthermore, these thermal analysis methods have the added advantage of being directly applicable to whole oil shale samples, which, except for crushing, need not be pretreated in any way. The potential problems of loss, alteration and the imperfections in removal or concentration processes are thus obviated [8]. Conversely, specific concentrated samples are equally suitable for the application of these methods if required.

In the present study, the most commonly occurring members of the carbonate and clay mineral groups, together with quartz were used to illustrate the validity, potential and applications of the TG and DTA methods.

EXPERIMENTAL

In all cases artificial mixtures and content reductions (dilutant calcined alumina, Al_2O_3) were on a weight percent basis from material at $-150^\circ\text{BSS} (-75 \mu\text{m})$.

The curves of individual minerals and specific mineral dilution sequences (Figs. 1–5) were obtained using the older equipment described previously [9]. All the oil shale determinations (Figs. 6–13) were made with the new Stanton-Redcroft STA781 simultaneous TG/DTA unit using thin-walled platinum crucible sample holders, under controlled preselected furnace atmosphere conditions of oxygen, free N_2 and high purity CO_2 flowing at $50 \text{ cm}^3 \text{ min}^{-1}$, at ambient pressure, with a constant heating rate of $15^\circ \text{ min}^{-1}$.

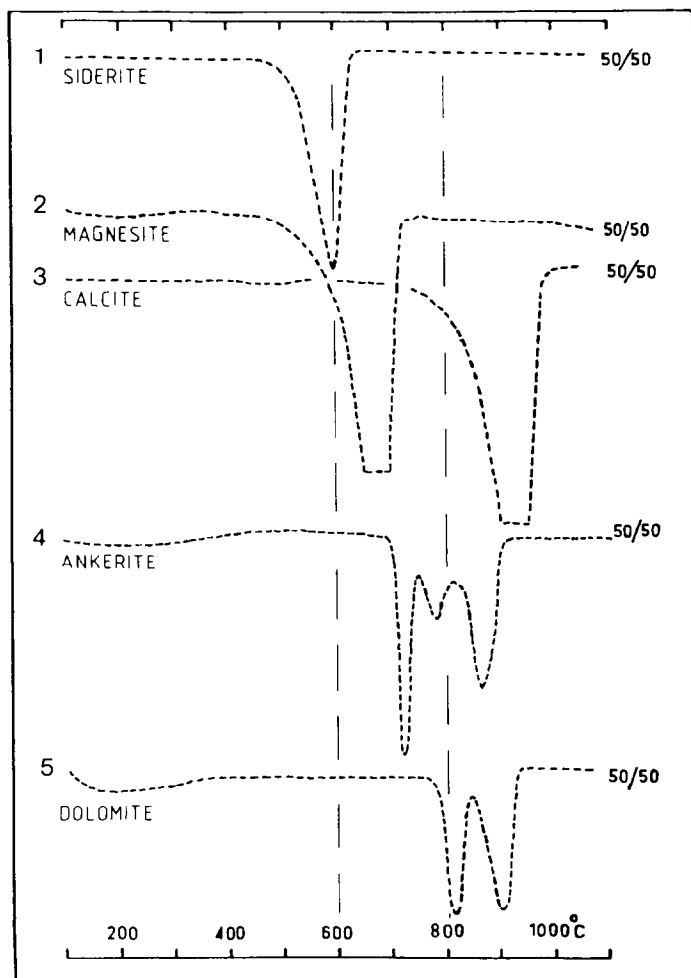


Fig. 1. DTA curves of selected anhydrous carbonate minerals, determined in flowing N_2 from powdered samples diluted with 50% Al_2O_3 .

Preselected recording sensitivities and ranges were: DTA, 100 μv and TG, 30-mg samples with 50% full scale deflection.

RESULTS

Furnace atmosphere conditions

The burning effects of heating coal and oil shale in air have been successfully suppressed by using an inert atmosphere of flowing N_2 , in order to apply TG to routine proximate analysis of coal [10,11], coal and coke [12], coal and oil shale [13,14], demineralised oil shales [15] and to the detection of minerals in whole coal samples [16,8]. This method has been used in the

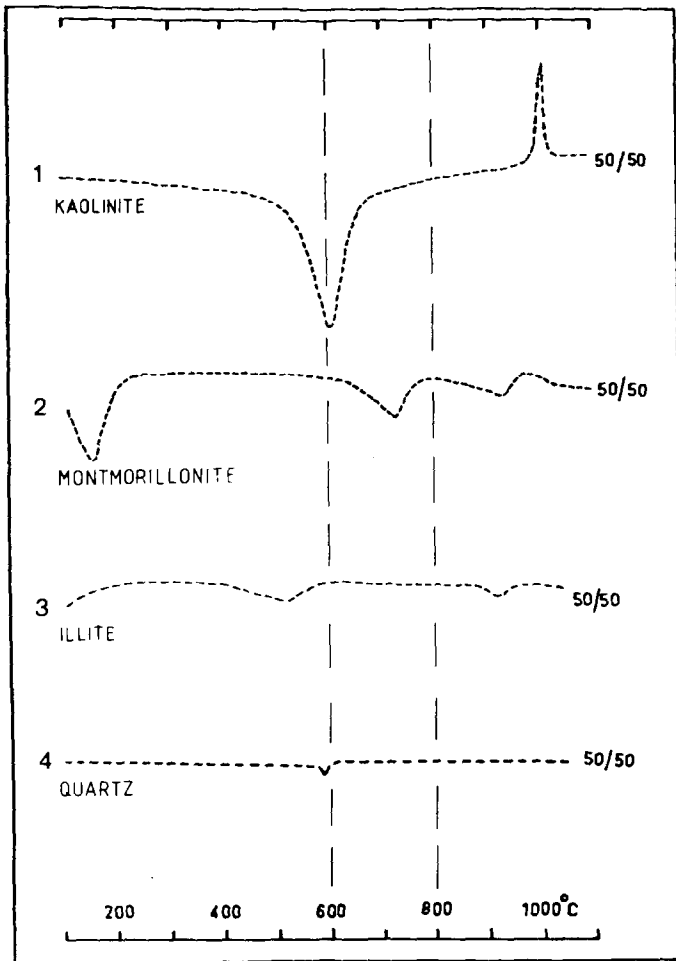


Fig. 2. DTA curves of selected clay minerals plus quartz, determined in flowing N_2 from powdered samples diluted with 50% Al_2O_3 .

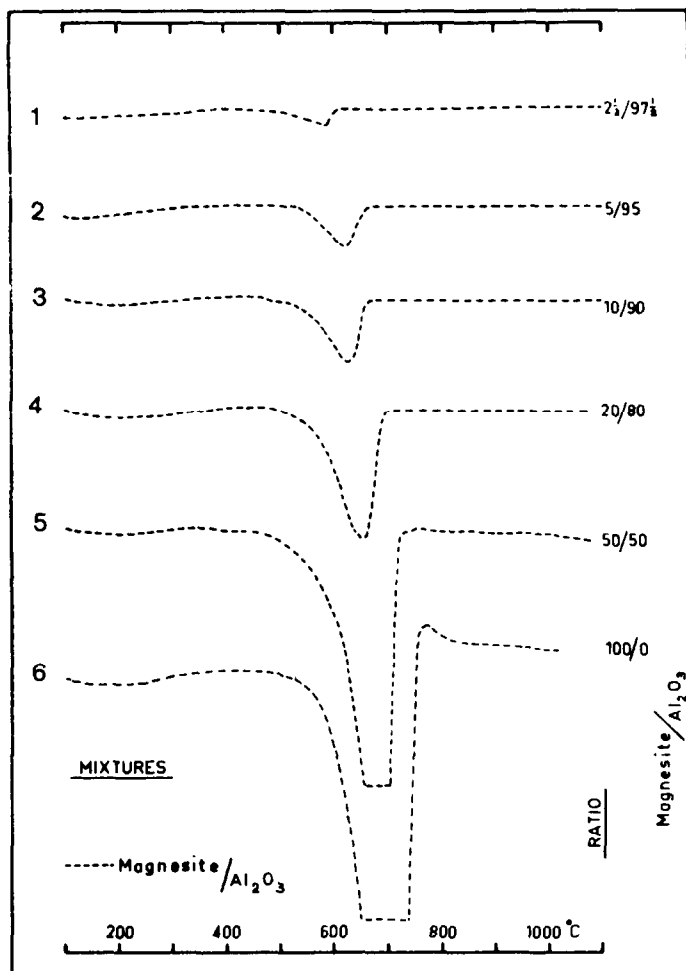


Fig. 3. Dilution sequence of DTA curves determined in flowing N₂ from magnesite/Al₂O₃ mixtures. Shows decreasing peak area, height and temperature with falling magnesite contents.

present study to establish reference TG and DTA curves from a suitable, untreated, low mineral content, low rank oil shale from Rundle, Australia. (This is the only oil shale material used in the study.) The oil shale was then mixed with 20% proportions of Al₂O₃ or individual minerals and subjected to thermal analysis. In this way mineral caused modifications to oil shale TG and DTA curves could be recorded, assessed and related directly to specific minerals.

Previous DTA work [7,9,18-20] had established that flowing furnace atmospheres of CO₂ were not only essentially inert (like N₂) but also produced predictable diagnostically useful and improved detection limit effects for carbonate minerals. Duplicate oil shale samples were therefore also run in this second gas (Figs. 6 and 7).

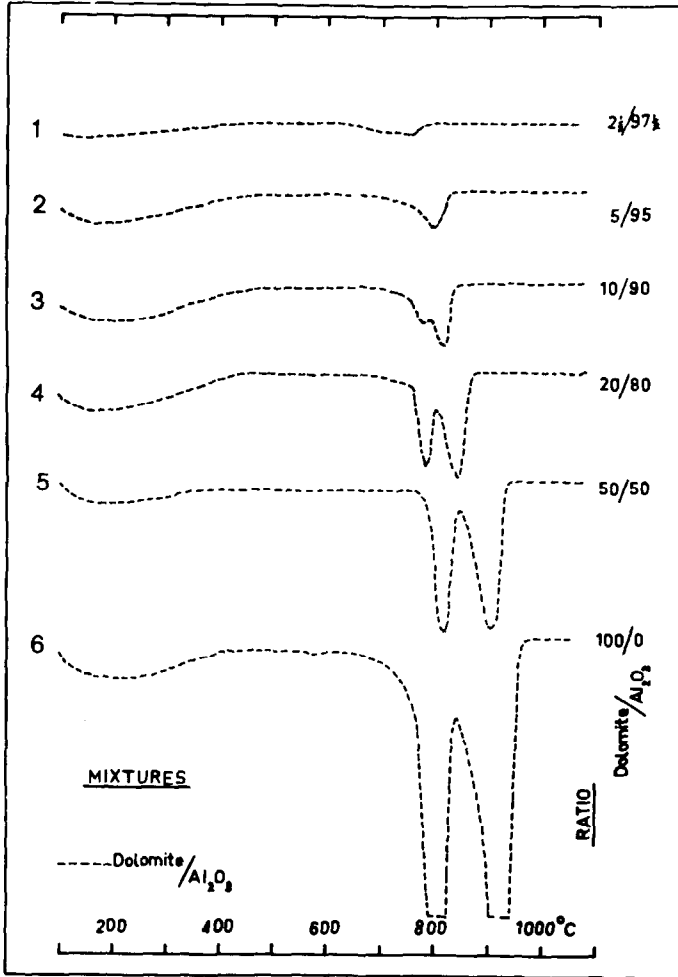


Fig. 4. Dilution sequence of DTA curves determined in flowing N_2 from dolomite/ Al_2O_3 mixtures. Shows decreasing peak area, height and temperature with falling dolomite contents.

Characteristic DTA curves of individual minerals in flowing N_2

From artificial mixtures of powdered samples of single minerals, diluted with 50% Al_2O_3 , DTA curves were obtained in flowing N_2 . The resultant curves from the mixtures containing siderite, magnesite, calcite, dolomite or ankerite are shown as curves 1–5 in Fig. 1. Comparable curves obtained from mixtures containing kaolinite, montmorillonite, illite and quartz appear as curves 1–4 in Fig. 2.

A comparison of these figures shows that DTA curves from individual minerals are diagnostically different, and exhibit almost exclusively endothermic (heat robbing) reactions of different intensities. These reactions also take place below 600, between 600 and 800 (relatable to retorting conditions) and above 800°C (see dotted 600 and 800°C reference lines Figs. 1 and 2).

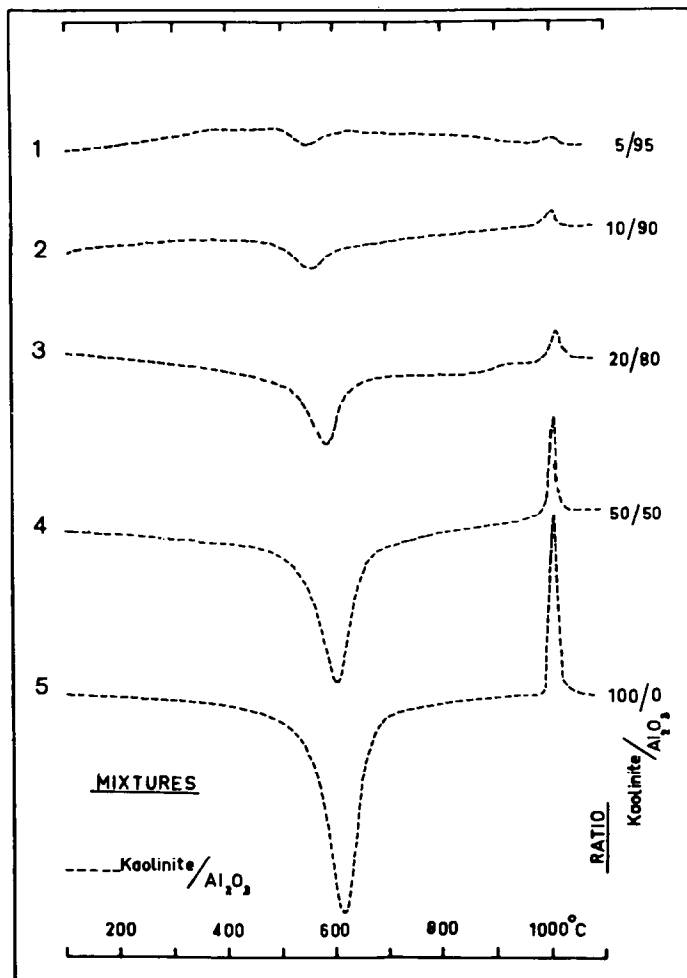


Fig. 5. Dilution sequence of DTA curves determined in flowing N_2 from kaolinite/ Al_2O_3 mixtures. Shows decreasing peak areas and heights with falling kaolinite contents, which also causes a decline in endothermic temperatures while those of the exothermic peaks remain unaffected.

Where these individual minerals exhibit more than one DTA reaction peak, this clearly indicates whether full decomposition has taken place or not, by a given temperature, e.g., in the case of dolomite at $\sim 800^\circ C$ (Fig. 1, curve 5) only the half calcination product (MgO) will have been liberated leaving $CaCO_3$ as compared to the full calcination products of MgO + CaO.

DTA dilution sequences of minerals in flowing N_2

Artificial dilution sequences of three minerals have been selected to illustrate different DTA curve modifications resulting in the drop in individ-

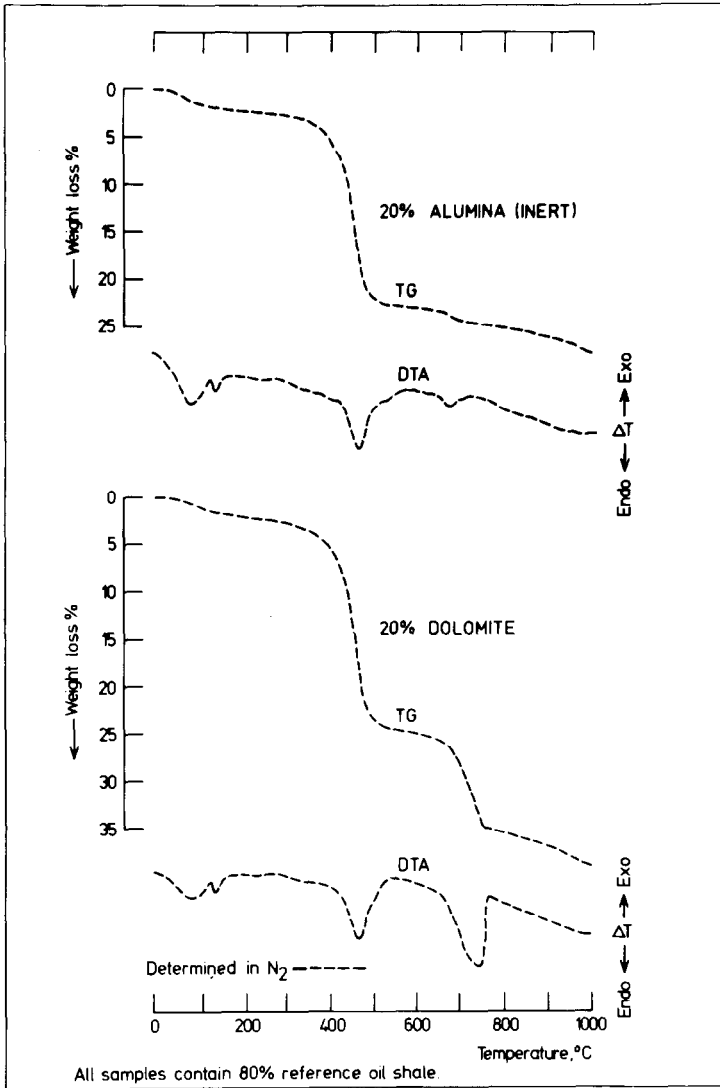


Fig. 6. Simultaneously determined TG and DTA curves obtained in flowing N_2 . The upper and lower pairs of curves are from duplicate samples of the oil shale diluted with 20% Al_2O_3 and dolomite, respectively.

ual mineral content. These are for magnesite (Fig. 3), dolomite (Fig. 4), and kaolinite (Fig. 5). For the single decomposition reaction mineral magnesite, Fig. 3 shows that as its content falls so does the peak area, height and temperature.

The same trends are shown by the double decomposition reaction mineral dolomite (Fig. 4). In addition, as dolomite contents fall the two characteristic DTA peaks progressively coalesce until they are represented by a single peak (Fig. 4).

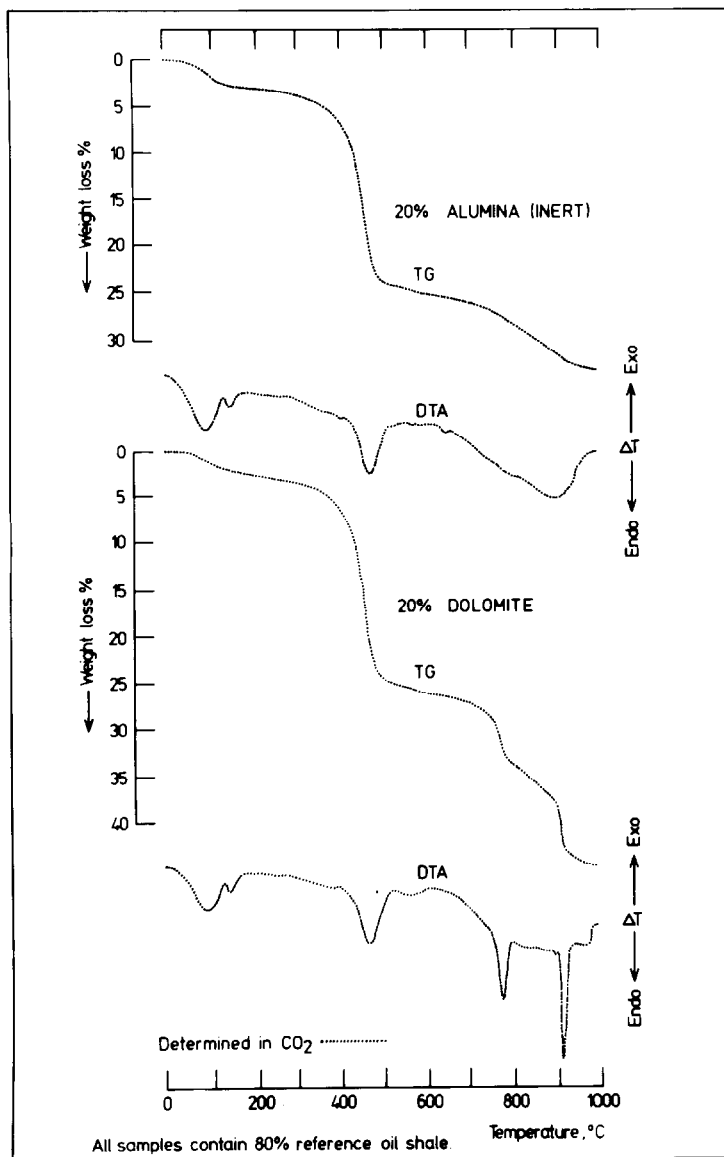


Fig. 7. Simultaneously determined TG and DTA curves obtained in flowing CO_2 . The upper and lower pairs of curves are from duplicate samples of the oil shale diluted with 20% Al_2O_3 and dolomite, respectively.

For kaolinite (Fig. 5) the “600°C” endothermic dehydroxylation peak again follows the same peak reduction trends. So also does the sharp “1000°C” exothermic peak, with the exception that its peak temperature remains virtually constant until the content has fallen below peak recognition levels.

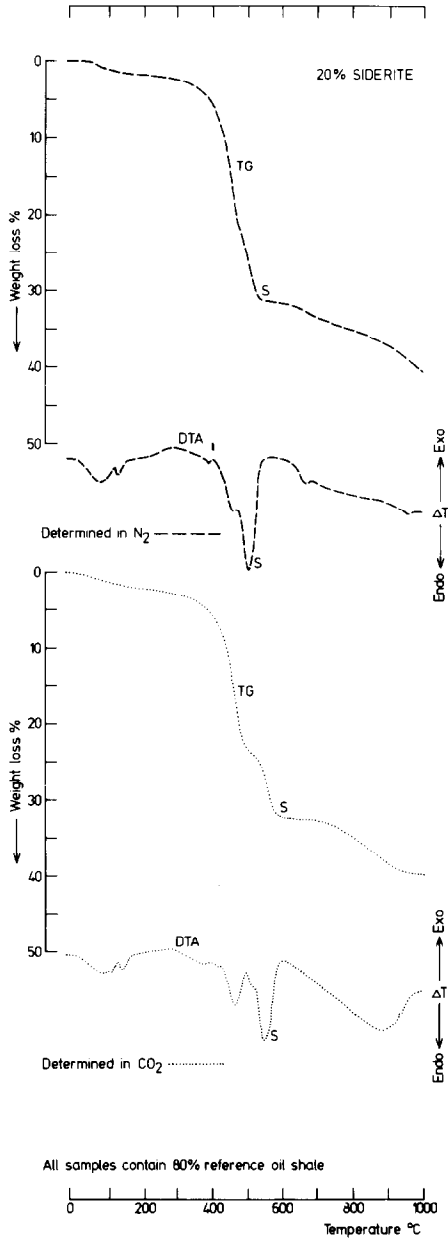


Fig. 8. Simultaneously determined TG and DTA curves obtained in flowing N₂ and CO₂ from duplicate samples of the oil shale diluted with 20% siderite.

Previously determined dilution sequences (similar to those in Figs. 3–5) for all the minerals studied herein established that the detection limits in N₂ are of the order of 1% for siderite, magnesite, calcite, dolomite and ankerite, and 2% for kaolinite. Conversely, dependent on crystallinity, montmoril-

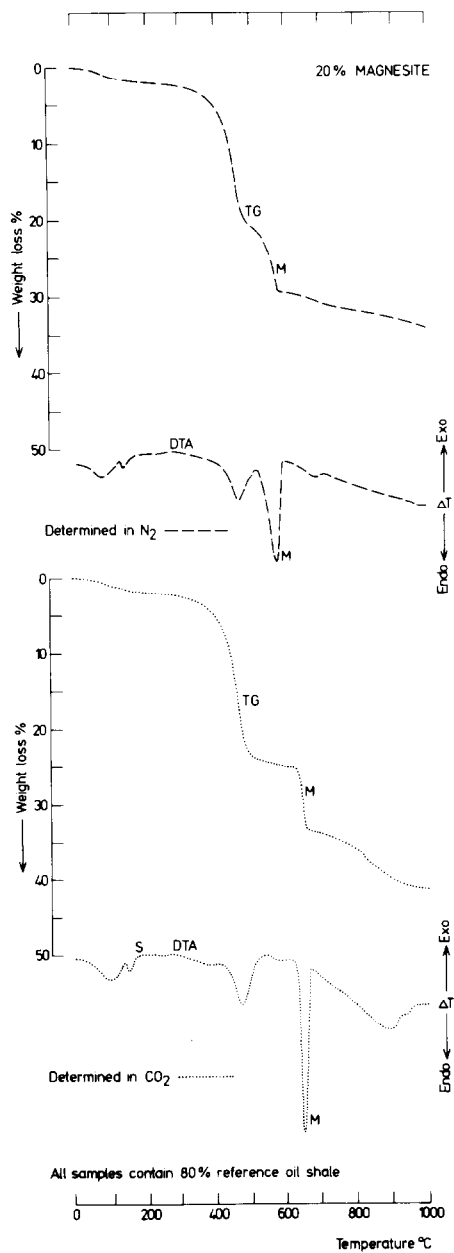


Fig. 9. Simultaneously determined TG and DTA curves obtained in flowing N₂ and CO₂ from duplicate samples of the oil shale diluted with 20% magnesite.

lonite, illite and quartz can only be detected if progressively greater amounts are present [16], i.e., ~ 15 and 30%, respectively. Because of its sharp peak, quartz may now be detectable in amounts as low as 2–5% with the latest

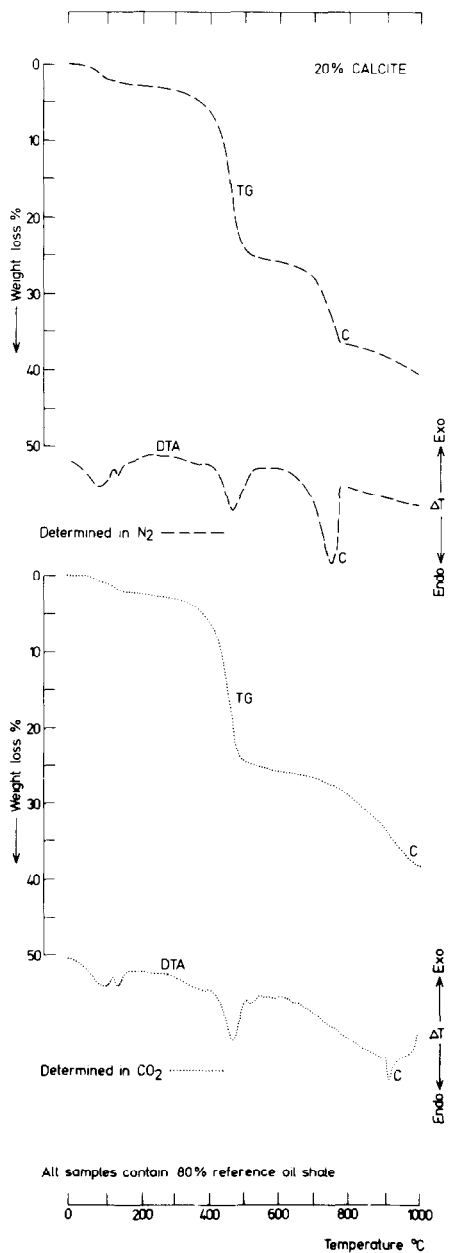


Fig. 10. Simultaneously determined TG and DTA curves obtained in flowing N₂ and CO₂ from duplicate samples of the oil shale diluted with 20% calcite.

high sensitivity equipment, but the mineral form in which this silica is present affects the resultant peak size [17].

Thus, the DTA method is best applied to the detection and evaluation of

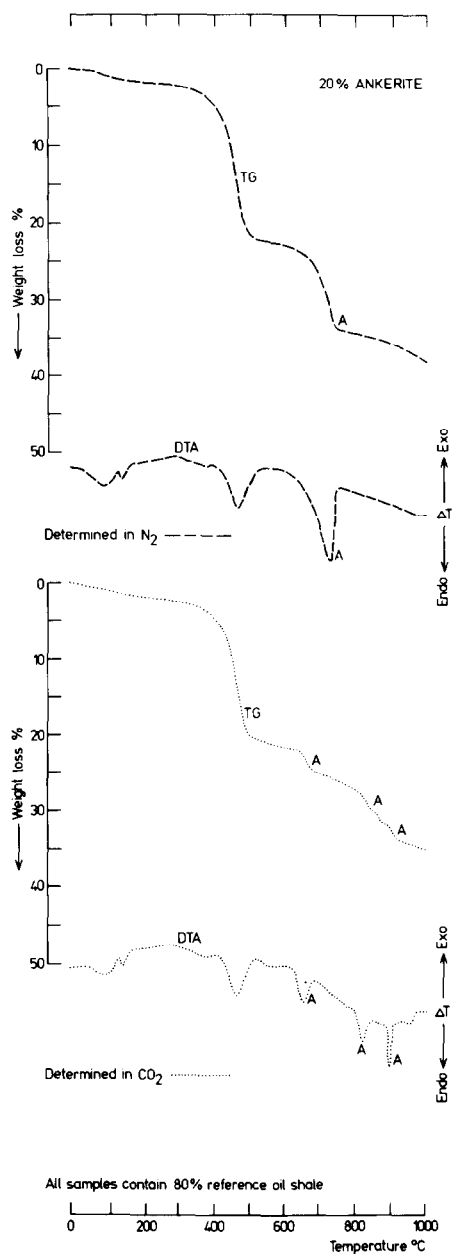


Fig. 11. Simultaneously determined TG and DTA curves obtained in flowing N₂ and CO₂ from duplicate samples of the oil shale diluted with 20% ankerite.

the carbonate group of minerals, whose detection limits may be extended down to contents in the order of 0.25%, if determined in conditions of flowing CO₂ [18].

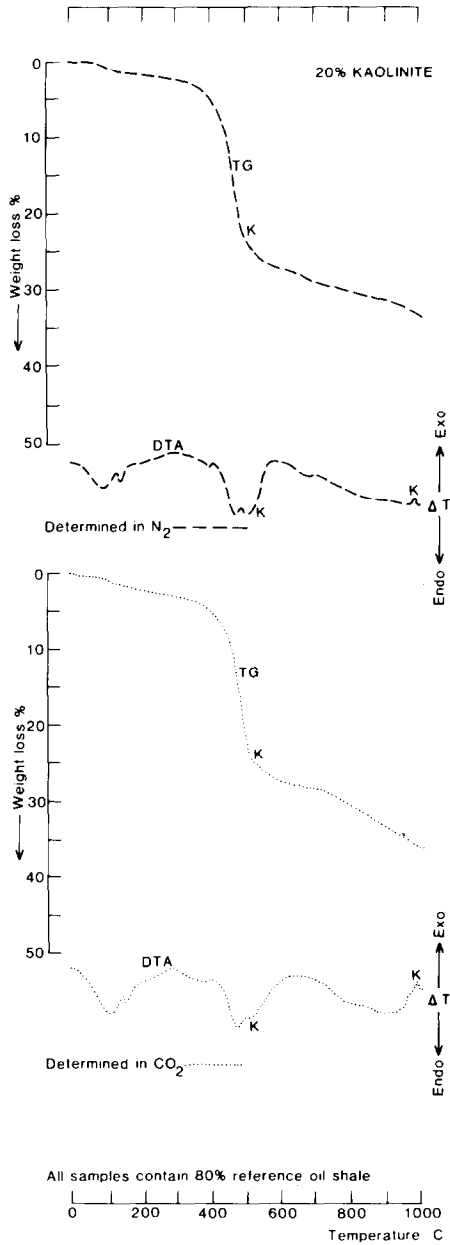


Fig. 12. Simultaneously determined TG and DTA curves obtained in flowing N_2 and CO_2 from duplicate samples of the oil shale diluted with 20% kaolinite.

Reference oil shale determinations in flowing N_2 and CO_2

Duplicate artificial mixtures of the low mineral content oil shale were determined under furnace atmosphere conditions of flowing N_2 and CO_2 (see upper two curves of Figs. 6 and 7).

The TG curves are similar showing, with increasing temperature, three well separated weight-loss regions due to the loss of water, hydrocarbon rich volatiles [10–15] and “high” temperature carbonate CO_2 , respectively.

The simultaneously determined DTA curves show directly temperature and reaction related endothermic peaks. The first of the pair of closely adjacent low temperature peaks is due to the release of adsorbed and clay associated water and the second due to the release of the water of crystallisation of gypsum. The medium temperature “450°C” peak is attributed to evolved hydrocarbon contents, while the higher temperature peak is due to the decomposition of a small content of calcite.

It is most important to note that the oil shale hydrocarbon volatile matter yield must also contain valueless non-hydrocarbon components liberated from any minerals present which decompose in this general temperature region. It is the nature, detection and amounts of these components and their origin from specific minerals present in oil shales which is discussed in detail below.

These unmodified oil shale TG and DTA curves determined in flowing N_2 and CO_2 (top half of Figs. 6 and 7) are not refigured and all subsequent oil shale mineral mixture curves should be referred to these to facilitate the evaluation of mineral-caused modifications.

Oil shale mineral mixture determinations in flowing N_2 and CO_2

Mineral-caused oil shale DTA and TG curve modifications were established from artificial mixtures of the oil shale and 20% of each of the minerals whose clearly defined DTA curves exhibited also good detection limits, i.e., siderite, magnesite, calcite, dolomite, ankerite, kaolinite and pyrite. Pyrite was included because previous DTA work on pyrite in coal had indicated that its decomposition reaction size in N_2 and CO_2 was comparable [16].

The mineral modified DTA curves determined in flowing N_2 and CO_2 are shown in Figs. 8–13 and the lower halves of Figs. 6 and 7. Compare these with oil shale only curves (top halves of Figs. 6 and 7).

The effects of siderite

The effects of siderite decomposition are superimposed on the upper part of the 350–550°C oil shale volatile evolution zone, shown on both the TG and DTA curves (Fig. 8). In N_2 these are quite recognisable but their superposition is too close for clear separation and accurate evaluation. In flowing CO_2 the increased CO_2 partial pressure involved delays the siderite decomposition until a higher temperature has been reached. Decomposition effects are therefore delayed and move up-scale (higher temperature) sufficiently for them to be almost separated from the oil shale volatile evolution effects on both TG and DTA curves. Thus, the heat and weight effects of siderite decomposition can be much more clearly identified and evaluated.

The variable atmosphere TG and DTA curves in Fig. 8 clearly establish the following.

(A) In flowing N_2 : (1) the siderite effects occur in the temperature zone 450–550°C; (2) the CO_2 from siderite decomposition is produced mainly within the volatile yield temperature zone of the oil shale; (3) this CO_2 contributes a valueless component to the oil shale volatile yield; (4) siderite CO_2 is liberated over a range of $\sim 100^\circ C$ and its commercial significance will depend on the content of this mineral; (5) the presence of siderite may be detected by the occurrence of its single well defined endothermic DTA peak and comparable TG weight loss and its content evaluated down to 1–2%; (6) the endothermic decomposition of siderite is heat absorbing. (However, in air, oxidation will immediately follow decomposition, with an overall moderately exothermic result [21].)

(B) In flowing CO_2 : (1) the siderite decomposition effects move up-scale $\sim 50^\circ C$; (2) the presence of siderite may be confirmed by the predictable up-scale movement, particularly of the more clearly defined DTA peak when determined in CO_2 compared to N_2 .

The effects of magnesite

The effects of magnesite decomposition are only superimposed on the very uppermost portion of the oil shale volatile evolution zone (Fig. 9). In N_2 these are more clearly recognisable than for siderite but separation is still not complete. In flowing CO_2 , however, similar up-scale movements occur and the decomposition effects become well separated from the oil shale effects on both the TG and DTA curves.

These magnesite features may therefore be accurately measured and evaluated free from oil shale interference effects.

The variable atmosphere TG and DTA curves in Fig. 9, clearly establish that the effects of magnesite are similar to those of siderite, but with the following comments.

(A) In flowing N_2 : the magnesite effects occur at a higher temperature range, i.e., 500–600°C, the magnesite CO_2 is also liberated over a 100°C range, but is only partly within the volatile yield zone of the oil shale used. Decomposition is again by a single reaction, which is endothermic under all different gas atmosphere conditions to give similar detection limits.

(B) In flowing CO_2 : the up-scale movements of the decomposition effects appears a little larger at $\sim 70^\circ C$ and is diagnostic of a carbonate mineral, and, at these temperatures, magnesite.

The effects of calcite

The effects of calcite decomposition are not superimposed on the volatile evolution temperature zone of the oil shale used (Fig. 10). In N_2 these are therefore more clearly recognisable than for siderite or magnesite and

measurement and assessment are not interfered with by conflicting oil shale effects.

In general the effects are similar to siderite and magnesite, modified as follows.

(A) In flowing N_2 : the calcite effects occur at a still higher temperature range, i.e., 680–780°C, with CO_2 again liberated over a 100°C range and well above the oil shale volatile evolution feature. The decomposition is by a single endothermic reaction under all atmospheres. This occurs at temperatures diagnostically above those of siderite or magnesite relative to which it has similar detection limits.

(B) In flowing CO_2 : here a more marked diagnostic up-scale movement, i.e., ~ 150°C, is accompanied by a marked reduction in the calcite peak size compared to its duplicate sample determination in N_2 (Fig. 10).

This somewhat disconcerting but diagnostically valuable feature has been confirmed by a number of check runs of other mixtures of calcite with this oil shale. Further investigations of this phenomenon are nearing completion and are intended for separate publication.

The effects of dolomite

The effects of dolomite (the double carbonate, $CaMg(CO_3)_2$) are not superimposed on the volatile evolution zone of the oil shale used (Figs. 6 and 7).

In N_2 the dolomite effect (Fig. 6) is similar to the TG and DTA curve modification produced by calcite and although it occurs at the somewhat lower temperature range of 650–750°C, the 100°C range and detection limits are the same.

(A) In flowing N_2 : although two decomposition steps are involved these coalesce in N_2 as dolomite content falls (Fig. 4). These are represented by a single endothermic feature (Fig. 6) which does not remain unmodified by other furnace atmosphere conditions [18].

(B) In flowing CO_2 : here new phenomena result whereby for all concentrations: (1) down to the limits of detection the characteristic two-endothermic-peaked DTA curve [18] and TG weight-loss areas are clearly defined and separated; (2) the actual parting (temperature separation) of the two reactions is increased as, although the upper temperature reaction moves up scale the lower one falls or remains at the same temperature (Fig. 7 and ref. 8).

Thus, the diagnostic two-peaked DTA configuration may always be obtained to distinguish dolomite from calcite with a somewhat increased detection limit.

Curves in CO_2 also show that dolomite may be distinguished from comparable content mixtures of calcite with magnesite. Although not illustrated such DTA peaks occur in the positions of these individual minerals (cf. DTA curves in CO_2 ; Figs. 7,9 and 10).

The effects of ankerite

The effects of ankerite (the triple carbonate, $\text{Ca}(\text{Mg,Fe})(\text{CO}_3)_2$) are not superimposed on the oil shale volatile evolution zone (Fig. 11).

In N_2 the ankerite effect is similar to that of dolomite and calcite but with a temperature range of 630–750°C, with an increased temperature spread of ~ 120°C and similar detection limits (cf. Figs. 6, 10 and 11).

(A) In flowing N_2 : although three decomposition steps are involved, these coalesce in N_2 as the ankerite content falls and are represented by a single endothermic feature (upper half of Fig. 11) which does not remain unaffected by different furnace atmospheres [18].

(B) In flowing CO_2 : here the modifications are similar to dolomite with the additions that: (1) the three diagnostic weight loss and endothermic reactions are clearly defined and separated; (2) the lowest temperature DTA peak moves down scale whilst the other two higher temperature peaks move up scale compared to the single peak position as determined in N_2 (cf. Fig. 11, lower and upper parts).

Thus, the three-peaked DTA configuration may always be obtained to distinguish ankerite from dolomite or calcite.

Recently published related work [20] has established that the middle DTA peak and associated weight loss increases with rising Fe content, which also causes the first decomposition reaction to occur at progressively lower temperatures.

The effects of kaolinite

The thermal effects of kaolinite are composed of two well-developed reactions shown on the DTA curve as one endotherm between 450 and 550°C and one sharper exotherm between 980 and 1010°C (Fig. 12). The endothermic feature is caused by kaolinite dehydroxylation and is accompanied by a TG curve weight-loss due to water evolution. The exothermic feature is not accompanied by any weight variation and is attributed to the recrystallisation of a spinel phase [17].

The variable atmosphere TG and DTA curves in Fig. 12 establish the following.

(1) In flowing N_2 : (1) the kaolinite decomposition reaction occurs in the temperature zone 450–550°C which is mainly within the oil shale volatile yield range; (2) this decomposition contributes over a range of ~ 100°C valueless H_2O vapour to the oil shale volatile yield; (3) the presence of kaolinite is indicated most conclusively by the presence of its DTA “1000°C” exothermic peak, as its endothermic peak may be obscured by the similar effects of oil shale, siderite and/or magnesite in the 450–600°C region; (4) the resultant of the two reactions of kaolinite is still considerably endothermic and will be even more so if the retorting temperature is too low to cause the exothermic recrystallisation.

(B) In flowing CO_2 : as neither N_2 or CO_2 gas atmospheres effect H_2O

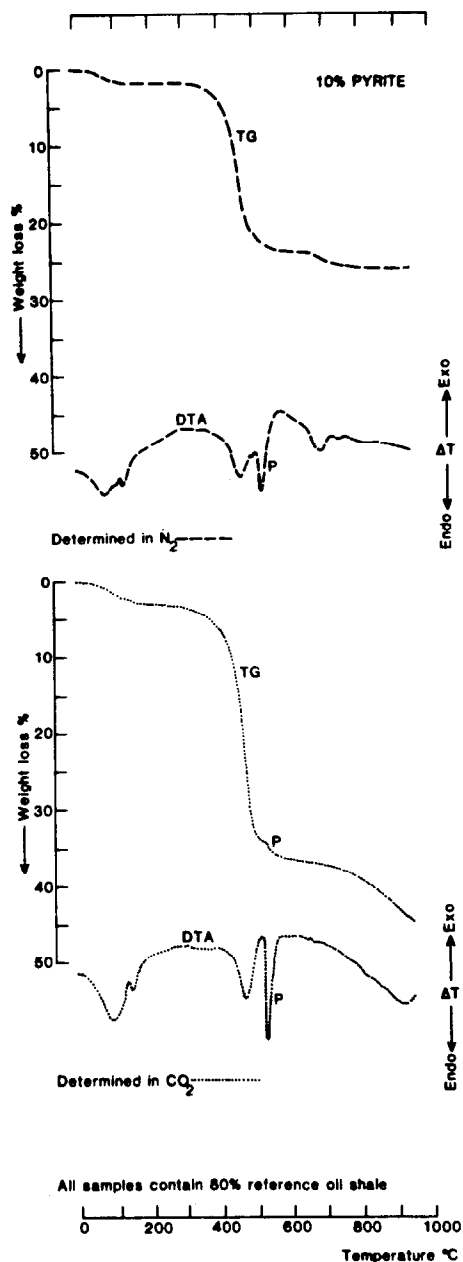


Fig. 13. Simultaneously determined TG and DTA curves obtained in flowing N_2 and CO_2 from duplicate samples of the oil shale diluted with 20% pyrite.

evolution or recrystallisation reactions, DTA curves of kaolinite are similar whichever gas is used.

However, the endothermic peak would be expected to move up scale in atmospheres of increased partial pressure of H_2O vapour.

The effects of pyrite

The effect of pyrite decomposition is superimposed on the uppermost part of the oil shale evolution zone (Fig. 13). In N_2 the DTA effect is clear but less well-developed than for siderite and magnesite, between which its decomposition peak lies. On the TG curve the weight-loss resulting from decomposition cannot be specifically identified or is lost within the oil shale volatile yield zone.

The single endothermic decomposition reaction of pyrite is followed immediately by exothermic oxidation peaks in the presence of oxygen. The configuration of these will depend on the degree of oxygen availability and the resultant heat balance is strongly exothermic under such conditions.

The variable atmosphere TG and DTA curves in Fig. 13 establish the following.

(A) In flowing N_2 : (1) the pyrite decomposition reaction occurs in the temperature zone 510–570°C which is within the oil shale volatile yield range; (2) this decomposition contributes over a range of ~ 60°C sulphur the presence of which in the oil shale volatile yield is detrimental; (3) the presence of pyrite may be detected by its single sharp endothermic decomposition peak and comparable TG weight loss and its content evaluated down to 1–2%; (4) the endothermic decomposition of pyrite in an inert atmosphere is heat absorbing and again robs heat from the retorting process. However, in air, oxidation will immediately follow to form the deleterious gases, SO_x . Such oxidation effects are very strong, thus, the overall resultant effect in air is strongly exothermic.

(B) In flowing CO_2 : as neither N_2 or CO_2 gas atmospheres affect the sulphide decomposition reaction, the TG and DTA effects should be comparable. However, in CO_2 the pyrite effects appear somewhat better defined although their temperature position remains constant. The improved resolution appears due to a slightly earlier completion of the hydrocarbon yield. (A similar effect is evident on the DTA curves of coal containing pyrite as determined in N_2 and CO_2 [22].)

DISCUSSION AND CONCLUSIONS

As the variable inorganic contents of oil shales are usually high (> 50%) the mineralogy is particularly important, due to the decomposition products released, their possible recombination and because of the endothermic or exothermic nature of the reactions involved. The magnitude of these reactions, assessable by TG and DTA, is applicable to retorting technology and deposit quality assessment.

Specifically, the common oil shale minerals examined herein have diagnostically different thermal effects which may be clearly identified and generally quantified from simultaneously determined DTA and TG curves.

The range of detection limits varies, but for many minerals it is at least 1–2%, while the anhydrous carbonate minerals together with kaolinite and pyrite are best suited for assessment by these methods.

Anhydrous carbonate mineral identification may be confirmed by their predictable DTA peak movements when determined in CO₂ compared to N₂. Carbonate, clay and sulphide minerals on decomposition produce the valueless gases CO₂, H₂O and SO_x, respectively, which in most cases will be produced in the oil shale or retorting temperature range.

The volatile matter yield temperature zone should be well characterised by TG/DTA for each oil shale deposit, as it may change laterally or from one seam to another in response to variations in kerogen type, rank and associated minerals.

For given maximum retorting temperature conditions TG and DTA will indicate the identity of the minerals and which will decompose at what temperatures, under various heating rates and atmosphere conditions. The type and magnitude of the associated endothermic and exothermic effects may also be assessed.

The availability of MgO and CaO (produced by separate decomposition reactions in dolomite and ankerite) for SO₂ fixation is temperature dependent under specific atmosphere conditions. Thus, MgO is released at a considerably lower temperature than CaO and at temperatures which are further reduced by progressive substitution of Fe for Mg in this mineral lattice. This, in turn, lessens the amount of MgO available from this mineral source as Fe substitution progresses.

In addition, these thermal analysis methods have the potential to provide a comparable method for the assessment of the effectiveness of oil shale beneficiation products, additives and catalysts.

ACKNOWLEDGEMENTS

This work forms part of a project on Low Rank Oil Shales, currently supported under the National Energy Research, Development and Demonstration Program, administered by the Commonwealth Department of National Development and Energy (Australia).

The Rundle Oil Shale sample used was kindly provided by Southern Pacific Petroleum NL and Central Pacific Minerals NL and we are indebted to Mrs. M. Shilcock, Mrs. J. Walker and Mr. W. Crebert for enthusiastic manuscript preparation, photography and drafting, respectively.

REFERENCES

- 1 A.C. Cook, A.J. Kantsler, A.C. Hutton and S.St.J. Warne, in A.C. Cook and A.J. Kantsler (Eds.), *Oil Shale Petrology Workshop*, Wollongong, 1980, Keiraville Kopiers, Wollongong, 1980, pp. 70–76.

- 2 J. Espitalie, M. Madec and B. Tissot, *Bull. Am. Assoc. Petrol. Geol.*, 64 (1980) 59.
- 3 S.St.J. Warne, in A.C. Cook and A.J. Kantsler (Eds.), *Oil Shale Petrology Workshop*, Wollongong, 1980, Keiraville Kopiers, Wollongong, 1980.
- 4 A.C. Hutton, A.J. Kantsler, A.C. Cook and D.M. McKirdy, *APEA J.*, 20 (1980) 44.
- 5 A.C. Cook, A.C. Hutton, A.J. Kantsler and S.St.J. Warne, *Sci. Aust.*, 4 (1980) 6.
- 6 C. Milton, *Wyo. Univ. Contrib. Geol.*, 10 (1971) 57.
- 7 S.St.J. Warne, *Proc. 6th Int. Conf. Therm. Anal.*, Bayreuth, Germany, 1980, Birkhaeuser Verlag, Stuttgart, pp. 283–288.
- 8 S.St.J. Warne, *Proc. 7th Int. Conf. Therm. Anal.*, Kingston, Canada, Vol. 2, 1982, Wiley, Chichester, pp. 1161–1174.
- 9 S.St.J. Warne, *J. Inst. Fuel*, 48 (1975) 142.
- 10 J.W. Cumming, in D. Dollimore (Ed.), *Proc. 2nd Euro. Symp. Therm. Anal.*, Aberdeen, Scotland, 1981, Heyden, London, pp. 512–516.
- 11 C.M. Earnest and R.L. Fyans, *Thermal Analysis Application Study No. 32*, Perkin-Elmer Corp., Norwalk, CT, U.S.A., 1981, p. 1.
- 12 M. Ottaway, *Fuel*, 61 (1982) 713.
- 13 J.P. Elder, in P.K. Agarwal (Ed.), *10th NATAS Conf.*, Boston, MA, U.S.A., 1980, Howard University Press, Washington, DC, pp. 247–253.
- 14 J.P. Elder, *Fuel*, 62 (1983) 580.
- 15 J.D. Saxby, *Thermochim. Acta*, 47 (1981) 121.
- 16 S.St.J. Warne, *J. Inst. Fuel*, 38 (1965) 207.
- 17 S.St.J. Warne, in Clarence Karr, Jr. (Ed.), *Analytical Methods for Coal and Coal Products*, Academic Press, London, 1979, pp. 447–477.
- 18 S.St.J. Warne, *Nature (London)*, 269 (1977) 678.
- 19 S.St.J. Warne, *Proc. 5th Int. Conf. Therm. Anal.*, Kyoto, Japan, 1977, Kagaka Gijyusu, Sha, distributed by Shuppan, Tokyo, Heyden, London, pp. 460–463.
- 20 S.St.J. Warne, D.J. Morgan and A.E. Milodowski, *Thermochim. Acta*, 51 (1981) 105.
- 21 S.St.J. Warne, *Chem. Erde*, 35 (1976) 251.
- 22 S.St.J. Warne, *J. Inst. Fuel*, 52 (1979) 21.